Subharmonic generation at interfaces of a thin layer between metal blocks

Takahiro Hayashi and Shiro Biwa

Graduate School of Engineering, Kyoto University,
Kyoto-daigaku Katsura, Nishikyo-ku, Kyoto 615-8540, Japan

Subharmonic wave was significantly generated at interfaces of aluminum blocks and an aluminum foil subjected to a 6 MHz burst incident wave. Although the fundamental wave amplitude was linearly varied with input voltage, subharmonic wave generated at the interfaces indicated strong nonlinearity. Analyzing the relationship of the subharmonic generation, the applied contact pressure and stress of ultrasonic wave has revealed that subharmonic components can generate when the incident ultrasonic wave has sufficiently large stress to separate the contacting interfaces. At rough surfaces, subharmonic peak could not be observed because large true contact pressure prevented the interfaces from separating.

E-mail address: hayashi@kuaero.kyoto-u.ac.jp

1. Introduction

Nonlinear ultrasonic nondestructive evaluation (NDE) has been widely studied as a new material evaluation technique in which material nonlinearity is detected from higher order harmonic or subharnomic waves[1-23]. The nonlinear ultrasonic NDE has the potential to detect micro cracks, inclusions and closed cracks that are supposed to be undetectable with conventional ultrasonic techniques. After Solodov[1] presented that relatively large nonlinear ultrasonic phenomana are generated at contacting interfaces, the new NDE technique has been studied aiming at precise evaluation of stress corrosion cracks and fatigue cracks.

Nonlinear phenomena at contacting interfaces were theoretically investigated by many researchers such as Richardson[2], Baik and Thompson[3], Pecorari[4], and Biwa *et al* [5]. Higher harmonic generation at interfaces was successfully modeled with dash-pot, spring-mass and/or nonlinear spring, which agreed well with the experimental results. However, for the subharmonic generation[6-15], theoretical studies and fundamental experiments are insufficient to explain the phenomena clearly.

This paper, therefore, discusses the mechanism of subharmonic generation from experimental results obtained for aluminum blocks with a thin aluminum foil.

2. Large subharmonic generation at a thin layer between metal blocks

Most of the previous studies on subharmonic generation in metallic materials deal with structures which vibrate with large displacements. For example, Solodov *et al*. [6] and Korshak *et al*. [7] discussed subharmonic generation at free boundaries of surface cracks on lithium niobate substrate and Delrue and Abeele[8] investigated a thin delamination region in a plate.

Based on these results, we introduced specimens consisting of two aluminum blocks and a sheet of aluminum foil, in which the aluminum foil could vibrate with large amplitude and induce subharmonic components as seen in the previous studies.

2.1 Experimental set-up and specimens

Figure 1 shows a schematic figure of experiments carried out in this study. Ultrasonic transducers placed on both sides of aluminum blocks (Olympus,V109, 5MHz central frequency) emit and receive waveforms transmitted through contacting interfaces which consist of an aluminum foil of 20 μm thickness and two aluminum blocks (A5052, 40mm × 50mm × 40mm). Sinusoidal burst signals of 6 MHz and 72 cycles were applied to the emitting ultrasonic transducer with various input voltage amplitudes by ultrasonic pulser (RITEC, RPR-4000). Hereafter the peak-to-peak input voltage is simply referred to as input voltage. Receiving signals in the other ultrasonic transducer were digitized by an AD board (National Instruments, USB-5133) with the sampling frequency of 50 MHz and recorded after signal averaging of 50 times.

The contact surfaces of aluminum blocks were polished by #180, #320, and #1000 emery papers, resulting in ten-point mean surface roughness *Rz* of about 7.9, 4.0, and 3.3 μm, respectively. From here, these aluminum blocks are named after the emery papers as #180, #320, and #1000 blocks. The aluminum foil has *Rz* of about 1.7 and 2.7 μm for glossy and frosted surfaces, respectively.

Compressive forces were applied to the aluminum blocks with a vice and measured by a load cell to calculate the nominal applied pressure. The transducers were adhered to the aluminum blocks with constant force using the jig and sponges as shown in Fig.1.

2.2 Typical waveform and amplitude spectrum

Figure 2 shows the transmitted waveforms in the #1000 blocks with an aluminum foil at nominal contact pressure of 0.064 MPa. Signal applied to the transmitter was a 6 MHz, 72-cycle burst wave with the input voltage of 370 V. The first wave packet between 15 μs and 28 μs is the direct transmitted wave, and the second one from 28 μs to 41 μs is a wave reflected once each at the interface and the block end, whose path is 80 mm longer than the direct transmitted wave. The third one after 41 μs is a wave reflected twice each at them, whose path is 160 mm longer. The first wave packet is partially zoomed in the inset, which shows that peaks repeat up and down. This is the characteristic of a signal containing subharmonic wave of a half driving frequency.

Figure 3 shows amplitude spectra obtained by discrete Fourier transform after applying a Hamming window function in the time range of direct transmitted wave (17.0 μs - 26.6 μs) and zero-padding all data except the time range. Figure 3 (a) represents the amplitude spectrum for the blocks with an aluminum foil. For comparison, the amplitude spectra are shown in (b) and (c) for those without an aluminum foil and one block (40 mm × 50 mm × 80mm) that has no interfaces. In (c), the receiving signals were reduced by an attenuator in 20 dB to avoid saturation of the large signals.

The figure shows that subharmonic wave was detected in the specimen with an aluminum foil (a), but not detected in that without an aluminum foil (b) and in that with no interfaces (c).

To clarify the relationship between the input voltage to the transmitter and the displacement of incident wave, we measured surface displacement with Laser Doppler vibrometer (Ono-Sokki, LV-1720 with 20MHz wide range unit LV-0160) for one block

(40 mm × 50 mm × 40 mm). Figure 4 is the waveform for 6 MHz and the input voltage of 347 V in displacement representation, which was obtained by integrating waveforms in velocity representation detected with the Laser Doppler vibrometer. Before the integration, measured signals were filtered by a Chebyshev high-pass filter with a cutoff frequency of 2 MHz to avoid monotonic drift owing to DC and low frequency errors in the measurement system. The first large pulse was neglected because it appeared as the result of integration error in the burst signals, and the displacement amplitude was determined to be about 5 nm from the subsequent burst amplitude shown in the figure. The amplitudes of displacement for various input voltages were obtained as Fig.5. The measured data can be approximated by a straight line passing through the origin with the slope of 1.465×10^{-2}. Since experiments were carried out in the range of input voltage below 500 V in this study, the maximum displacement is about 7.4 nm. This result indicates that subharmonic wave is generated at the interfaces of the blocks and the thin layer with relatively small incident wave displacement compared to the previous experiments[9-15].

3. Relationship of subharmonic generation with input voltage, contact pressure, and surface roughness

In this section, measured subharmonic amplitude (written as $A_{1/2}$) is shown for various input voltages, contact pressures, and surface roughness to discuss subharmonic generation at contacting interfaces.

3.1 Amplitude spectra and subharmonic amplitude change for various input voltage

Figure 6 shows the amplitude spectra for four different input voltages and the contact pressure of 0.26 MPa in #1000 blocks with the aluminum foil, which were

calculated using the same time gate and window function. Distinct subharmonic peaks can be seen at 3 MHz in (b), (c) and (d), while such a peak did not appear in the low input voltage as (a).

The difference between the subharmonic amplitude ($A_{1/2}$) and fundamental amplitude (A_1) in dB representation denotes the ratio of $A_{1/2}$ against A_1 as $A_{1/2}\ [dB] - A_1\ [dB] = 20\log(A_{1/2}/A_1)$. The relative subharmonic amplitudes were obtained for various input voltages and the four different contact pressures as shown in Fig.7. The upper horizontal axis represents an estimated internal ultrasonic stress as described later. The hatched region denotes that distinct subharmonic peaks were not observed. Since contact area became relatively small in the smallest contact pressure of 0.064 MPa, the transmitted fundamental wave amplitude A_1 was small in the low input voltage below 100 V. Therefore, the relative subharmonic amplitude became large even in the hatched area.

In the low contact pressures of 0.064 MPa and 0.26 MPa where remarkably large subharmonic amplitude was observed, the subharmonic component abruptly appeared beyond a certain input voltage, and then their abrupt increases were observed at higher voltages. For example, in 0.064 MPa, the subharmonic amplitude suddenly appears at about 100 V, and then the next sudden increase starts from about 230 V. The nonlinear behaviors at contacting interfaces like this were also obtained in the previous studies by Solodov[1, 6] and Ohara et al.[11, 12]

3.2 Subharmonic generation for various contact pressure

Prior to the discussion of the effect of contact pressure in subharmonic generation, the relationship between the input voltage and the internal stress of incident

wave is described.

In Fig.5, we obtained the relationship between ultrasonic amplitude and input voltage to the transmitted transducer. Considering that the normal displacement measured on free boundaries is the double of that in the medium, the maximum displacement of the ultrasonic wave propagating in the medium $u_{\max}$ [nm] can be estimated by dividing the equation in Fig.5 by two as,

$$u_{\max} = 1.465/2 \times 10^{-2} E, \tag{1}$$

where E [V] is the input voltage. Letting one-dimensional harmonic plane longitudinal wave be $u = u_{\max} \exp\{i\omega(x/c - t)\}$ with the use of a maximum displacement $u_{\max}$, ultrasonic velocity c, and angular frequency ω, ultrasonic stress σ can be represented as,

$$\begin{aligned}\sigma &= (\lambda + 2\mu)\frac{\partial u}{\partial x} \\ &= (\lambda + 2\mu)(i\omega/c)u_{\max} \exp\{i\omega(x/c - t)\} \\ &= i\rho c\omega u_{\max} \exp\{i\omega(x/c - t)\} \\ &= 2i\pi\rho c f u_{\max} \exp\{i\omega(x/c - t)\},\end{aligned} \tag{2}$$

where λ and μ are Lamé's constants, and ρ and f are density and frequency, respectively. From eq. (2), the relationship between the maximum ultrasonic stress $\sigma_{\max}$ and the maximum displacement $u_{\max}$ is derived as,

$$\sigma_{\max} = 2\pi\rho c f u_{\max}. \tag{3}$$

Substituting eq. (1) into eq. (3) gives the relationship between the input voltage E and the estimated internal maximum stress by ultrasonic wave $\sigma_{\max}$ as,

$$\sigma_{\max} = 4.77 \times 10^{-3} E, \tag{4}$$

where ρ=2700 kg/m^3, c=6400 m/s and f=6 MHz, and units of $\sigma_{\max}$ and E are MPa and V, respectively.

The upper horizontal axis in Fig.7 represents the estimated ultrasonic maximum stress obtained by eq. (4). For high contact pressures of 0.86 MPa and 1.70 MPa, subharmonic peak could not be detected clearly, while for the low contact pressures of 0.064 MPa and 0.26 MPa, the subharmonic peak could be detected beyond about 100 V and 160 V (0.48 MPa and 0.76 MPa of ultrasonic stress), respectively. This tendency agrees well with the previous studies on the relationship between contact pressure and nonlinear subharmonic generation[1), 6)], in which the authors explained that subharmonic wave generates as a result of interface opening induced by ultrasonic tensile stress and interface closing, that is called “clapping”.

3.3 Subharmonic generation for various surface roughnesses

Variations of the relative subharmonic amplitude with the input voltage are shown for three different surface roughnesses at the contact pressure of 0.064 MPa in Fig.8. This figure manifests that the relative subharmonic amplitude is totally different depending on surface roughness. For the flat surface of #1000, significantly large subharmonic peaks were obtained, while for the rough surface of #180, the subharmonic peak could not be observed.

We can also explain this qualitatively from the relationship between the contact pressure and internal stress of ultrasonic wave. Since the true contact area is much smaller than the nominal contact area in the rough surface, the true contact stress becomes much larger than the nominal contact pressure. Therefore, “clapping” at the rough interface did not occur as easily as at the flat interface, and subharmonic peaks could not be observed in #180.

4. Direct measurements of the aluminum foil interface

From the previous studies and the experimental results shown above, it is conceivable that subharmonic components are generated by the mixture of forced vibration of ultrasonic wave in interface-adhering phase and free vibration in separating phase of the interfaces. In the results shown above, the subharmonic components can generate only when an aluminum foil was inserted between aluminum blocks, and we can estimate that large free vibration occurs at the aluminum foil. Therefore, the vibration at the aluminum foil was measured directly with the laser Doppler vibrometer by replacing one aluminum block with a transparent acrylic resin block.

Figure 9 is a schematic figure of the experiments. Burst wave of 6MHz, 72 cycles was incident from the side surface of the #1000 aluminum block. The input voltage was 365 V, corresponding to the estimated ultrasonic stress of 1.74 MPa. Vibration on the aluminum foil at the interface with acrylic resin (Rz=0.9) was measured with the laser Doppler vibrometer, and was recorded after signal averaging of 100 times. Here, surface vibration for various contact pressures was measured as done above. Although the contact state was not identical to the previous experiments even in the same contact pressure, qualitative discussion is possible.

Figure 10 shows the waveforms at the aluminum foil and their amplitude spectra. The upper five waveforms and spectra (a)-(e) are the results when aluminum foil was inserted between acrylic and aluminum blocks as shown in Fig.9 and contact pressure was increased from (a) to (e) as shown in the figure. For comparison, (f) and (g) show the results for one aluminum block and blocks without aluminum foil, respectively.

Both in (f) and (g), the waveforms are very similar to the input burst signals

and their amplitudes are approximately the same. In (a)-(e), in which vibration on the aluminum foil was measured, the waveforms significantly differ by contact pressures. This is caused by the change of the mixture rate of forced and free vibrations at the interfaces. In (c) where the maximum amplitude was obtained, the aluminum block was adhered with the aluminum foil sufficiently for transmitting ultrasonic energy to the aluminum foil, and the aluminum foil was effectively separated from the acrylic block for large free vibration. In the case of (a)-(d) where large amplitude was observed, the subharmonic peaks can be obtained in the amplitude spectra, while in (e) for the highest contact pressure, the waveform was very similar to (g) and (f), and the subharmonic peak cannot be seen in the spectrum. This is because high contact pressure restricted the vibration of the aluminum foil.

5. Discussions on experimental results

In the experimental results, we observed occurrence of the subharmonic component of 3 MHz and their nonlinear behaviors such as the existence of certain thresholds and quasi-chaotic waveforms when 6 MHz burst wave was incident to the contacting interfaces between two aluminum blocks and a sheet of aluminum foil. Moreover, the relative amplitude was measured for various ultrasonic wave stress, contact pressure, and surface roughness, which showed that the relationship between true contact pressure and ultrasonic stress strongly affects the “clapping” phenomenon at the contacting interfaces.

Similar results were obtained in the previous studies for contacting interfaces of two metal rods and fatigue cracks by Solodov[1, 6, 7] and Yamanaka[9 - 12]. In ref. 1, at an interface consisting of two cross-sections of metal rods, subharmonic vibration and

chaotic phenomena were observed for harmonic vibration of 300 Hz at a low contact pressure. Figures 7 and 10 gave similar results at a high frequency region of ultrasonic wave. Especially in Fig. 10 showing vibrations on the aluminum foil, the waveforms look like quasi-chaotic and the frequency spectra provided high amplitude below the fundamental frequency at low contact pressures (a) 0.064 MPa, and (b) 0.29 MPa.

In refs. 6 and 7, step-like thresholds of $n\omega/2$ subharmonic wave were experimentally confirmed using ultrasonic wave in the order of kilo hertz. Moreover, multiple thresholds of subharmonic wave were discussed in ref.7. Although this study also provided multiple abrupt changes of subharmonic amplitude as seen in Fig.7 and 8, they were not “step-like”. This is because local contact pressure is not homogeneous owing to surface roughness. Since higher frequency wave has smaller amplitude in the same amount of vibration energy, ultrasonic wave in the order of MHz is relatively sensitive to surface roughness compared with that in kHz range. In this study, surface roughness of the aluminum foil and aluminum blocks ranging from Rz = 1.7 to 7.9 μm was much greater than the maximum ultrasonic amplitude 7.5 nm.

References 9 and 11 also presented the similar phenomena on subharmonic generation and amplitude change which were modeled by mass-spring with or without adhesion force. The thin layer introduced in this study may correspond to the mass of the model in the references.

The subharmonic generation shown in this study will support understanding of nonlinear ultrasonic behavior at contacting interfaces. Furthermore, it is expected to be applied to non-destructive evaluation for structures with a thin layer between solid media. The principal examples are stress corrosion cracks that include thin branched cracks at grain boundaries and liquid phase diffusion bonding using a thin insert

material.

6. Conclusions

In this study, large subharmonic generation was observed at the interfaces of aluminum blocks and an aluminum foil. Then, relative subharmonic amplitude was obtained for various input voltages, contact pressure, and surface roughness. Although fundamental wave amplitude was linearly varied with input voltages, subharmonic components generated at the interfaces indicated strong nonlinearity.

Analyzing the relationship of subharmonic generation, contact pressure and amplitude of ultrasonic wave has revealed that subharmonic wave can generate when the incident ultrasonic wave has sufficiently large stress to separate the contacting interfaces. Rough surfaces did not generate the subharmonic wave as true contact pressure at small contact area exceeded stress of incident wave.

Moreover, vibration on the aluminum foil was directly measured by laser Doppler vibrometer, which has revealed that displacement and subharmonic generation at the aluminum foil are strongly dependent on contact pressure.

References

1) I. Y. Solodov: Ultrasonics, **36** (1998) 383.

2) J. M. Richardson: Int. J. Eng. Sci., **17** (1979) 73.

3) J. Baik and R. B. Thompson: J. Nondestructive Evaluation, **4**, 3/4 (1984) 177.

4) C. Pecorari: J. Acoust. Soc. Am., **113**, 6 (2003) 3005.

5) S. Biwa, S. Nakajima, and N. Ohno: J. Appl. Mech., **71** (2004) 508.

6) I. Y. Solodov, N. Krohn, and G. Busse: Ultrasonics, **40** (2002) 621.

7) B. A. Korshak, I. Y. Solodov, and E. M. Ballad: Ultrasonics, **40** (2002) 707.

8) S. Delrue, and K. V. D. Abeele, Ultrasonics: **52** (2012) 315.

9) K. Yamanaka, T. Mihara, and T. Tsuji: Jpn. J. Appl. Phys. **43**, 5B (2004) 3067.

10) R. Sasaki, T. Ogata, Y. Ohara, T. Mihara, and K. Yamanaka: Jpn. J. Appl. Phys. **44** (2005), 4389.

11) Y. Ohara, T. Mihara, and K. Yamanaka: Ultrasonics, **44** (2006) 194.

12) Y. Ohara, S. Yamamoto, T. Mihara, and K. Yamanaka: Jpn. J. Appl. Phys. **47** (2008) 3908.

13) Y. Ohara, H. Endo, T. Mihara, and K. Yamanaka: Jpn. J. Appl. Phys. **48** (2009) 07GD01.

14) S. Horinouchu, M. Ikeuchi, Y. Shintaku, Y. Ohara, and K. Yamanaka: Jpn. J. Appl. Phys. **51** (2012) 07GB15.

15) Y. Ohara, Y. Shintaku, S. Horinouchi, M. Ikeuchi, and K. Yamanaka: Jpn. J. Appl. Phys. **51** (2012) 07GB18.

16) Y. Ohara, and K. Kawashima: Jpn. J. Appl. Phys. **43** (2004) 3119.

17) T. Ohtani, K. Kawashima, M. Drew, and P. Guagliard: Jpn. J. Appl. Phys. **46** (2007) 4557.

18) T. Ohtani, H. Ogi, and M Hirao: Jpn. J. Appl. Phys. **48** (2009) 07GD02.

19) C. Inserra, S. Biwa, and Y. Chen: Jpn. J. Appl. Phys. **48** (2009) 07GD03.

20) K. Kawashima, T. Ito, and Y. Nagata: Jpn. J. Appl. Phys. **49** (2010) 07HC11.

21) K. Kawashima: Jpn. J. Appl. Phys. **50** (2011) 07HC14.

22) M. Fukuda, and K. Imano, Jpn. J. Appl. Phys. **51** (2012) 07GB05.

23) N. Matsuda, and S. Biwa, Jpn. J. Appl. Phys. **51** (2012) 07GB14.

Figure Captions

Fig. 1. Schematic figure of experiments.

Fig. 2. Typical waveform for aluminum blocks (#1000) with an aluminum foil (Zoomed waveform is in the inset).

Fig. 3. Typical amplitude spectrum showing the difference of detected signals with and without an aluminum foil.

Fig. 4. Transient displacement at the end wall of one aluminum block.

Fig. 5. Relationship between input voltage and displacement.

Fig. 6. Amplitude spectra for various input voltages.
(#1000 blocks with aluminum foil, contact pressure 0.26MPa).

Fig. 7. Input voltage versus relative subharmonic amplitude
for various contact pressures. (#1000 blocks with aluminum foil).

Fig. 8. Input voltage versus relative subharmonic amplitude for various surface roughnesses.（specimens with aluminum foil, contact pressure 0.064MPa）.

Fig. 9. Schematic figure of measurements of interface vibration.

Fig. 10. Waveforms and amplitude spectra for various interface conditions.

Fig. 1. Schematic figure of experiments.

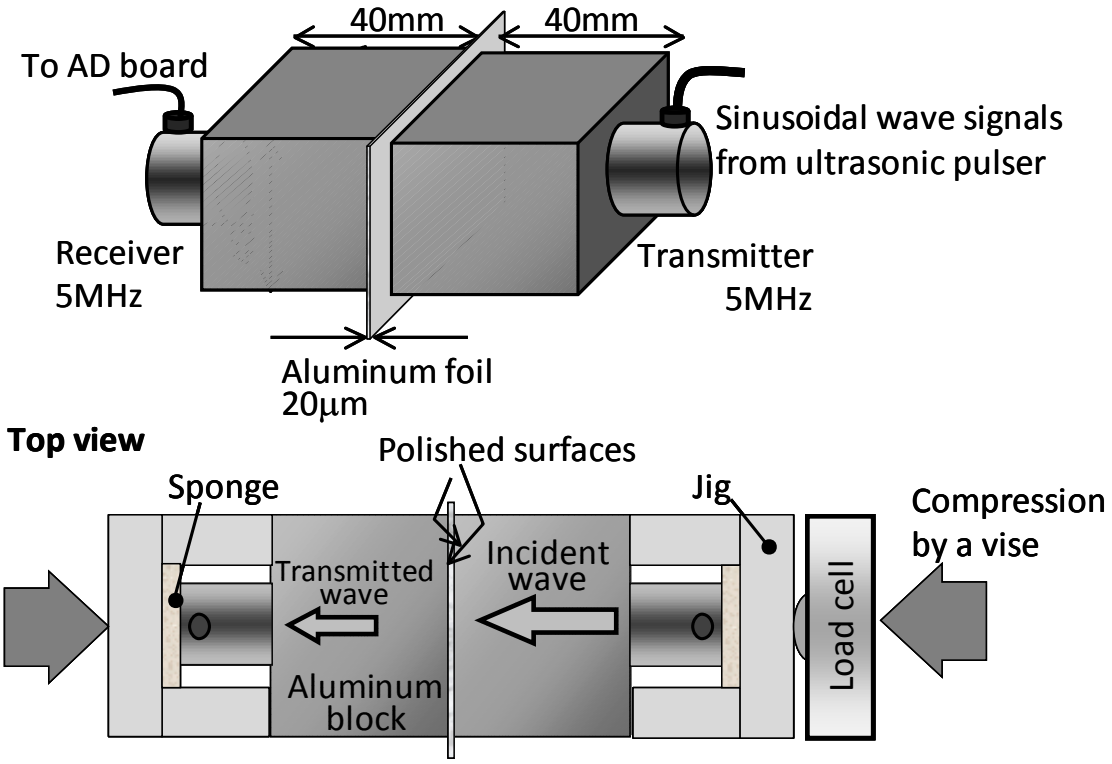

Fig. 2. Typical waveform for aluminum blocks (#1000) with an aluminum foil (Zoomed waveform is in the inset)

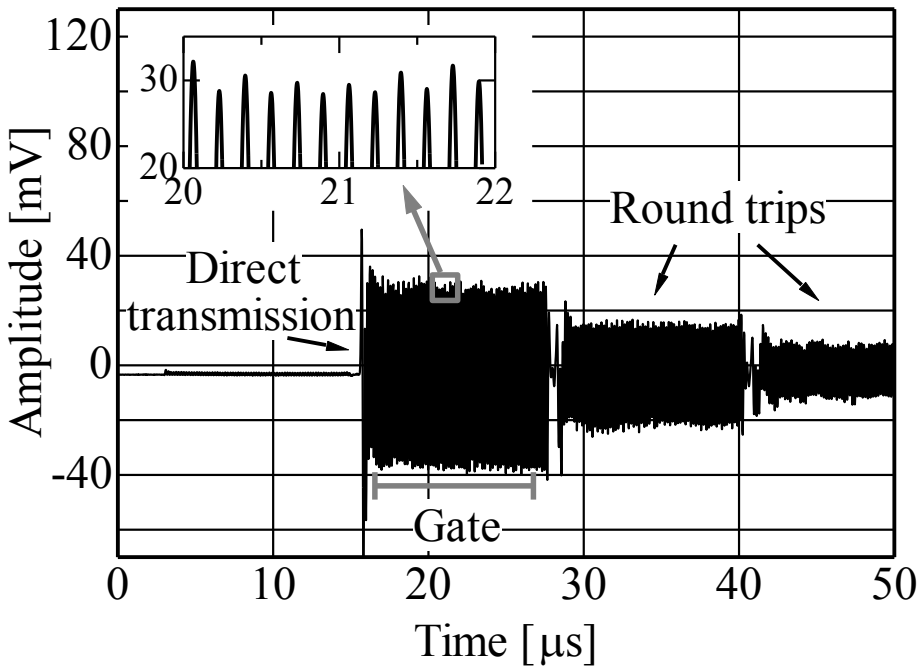

Fig. 3. Typical amplitude spectrum showing the difference of detected signals with and without an aluminum foil.

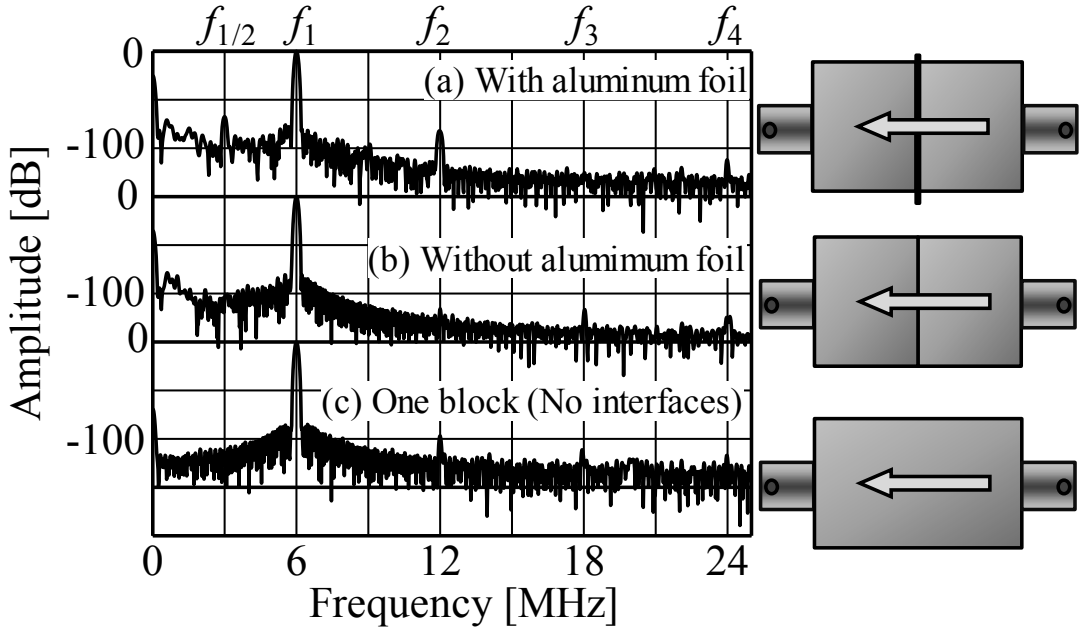

Fig. 4. Transient displacement at the end wall of one aluminum block

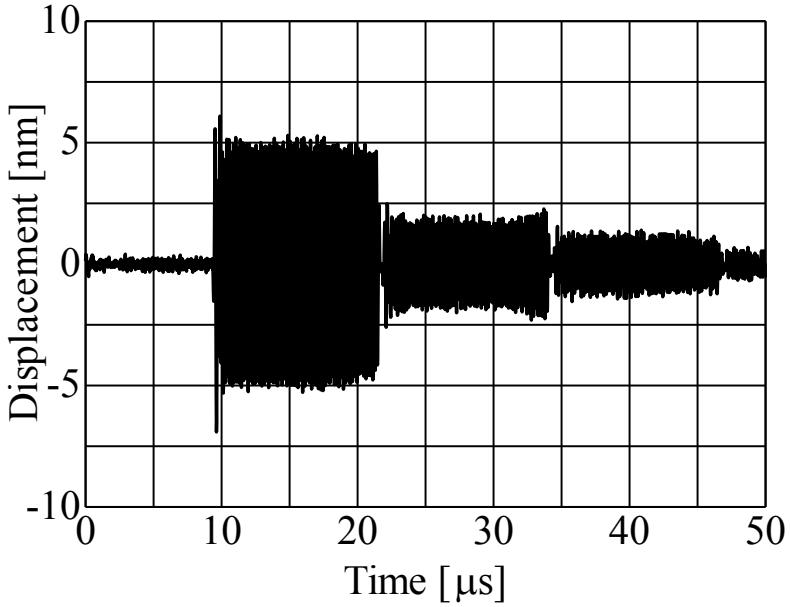

Fig. 5. Relationship between input voltage and displacement.

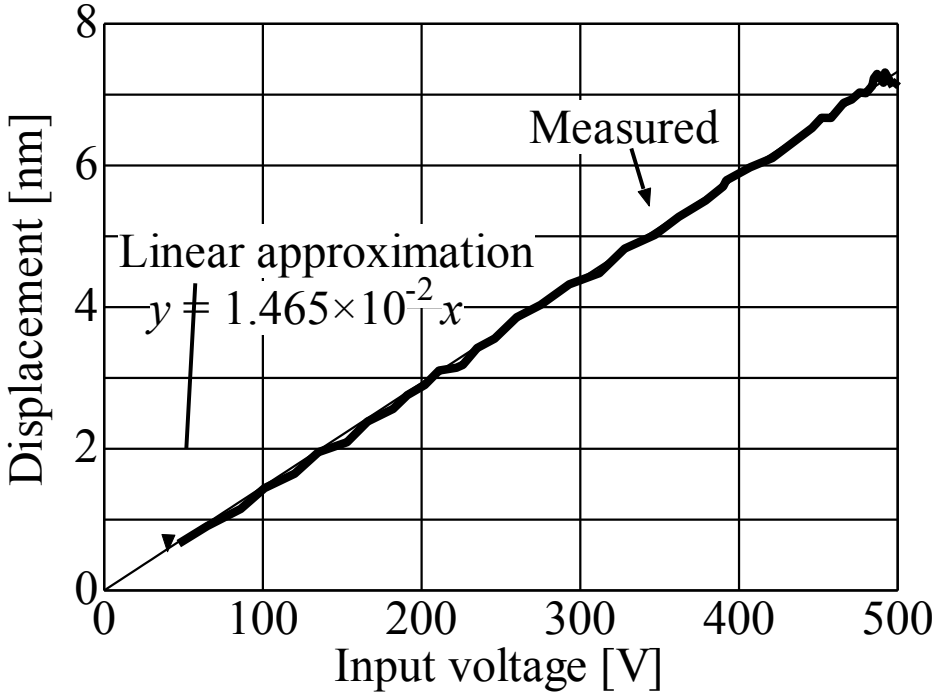

Fig. 6. Amplitude spectra for various input voltages.

(#1000 blocks with aluminum foil, contact pressure 0.26MPa).

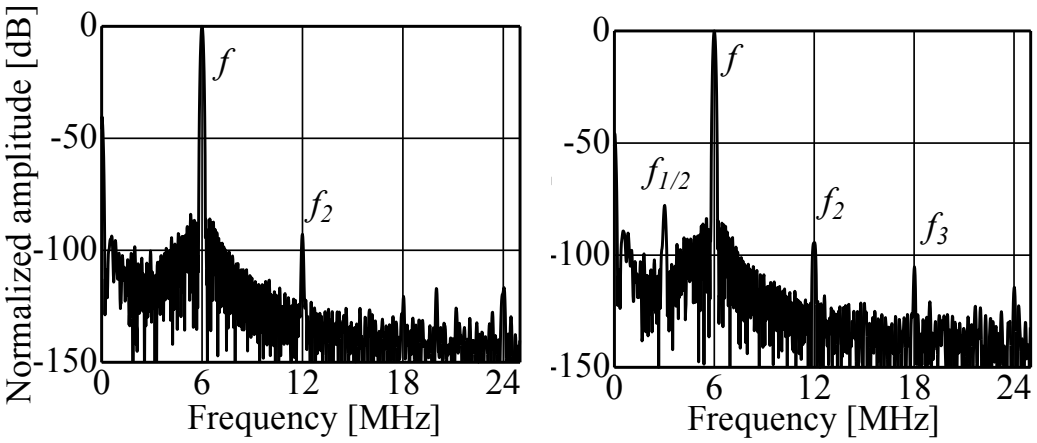

(a)101V (b) 206V

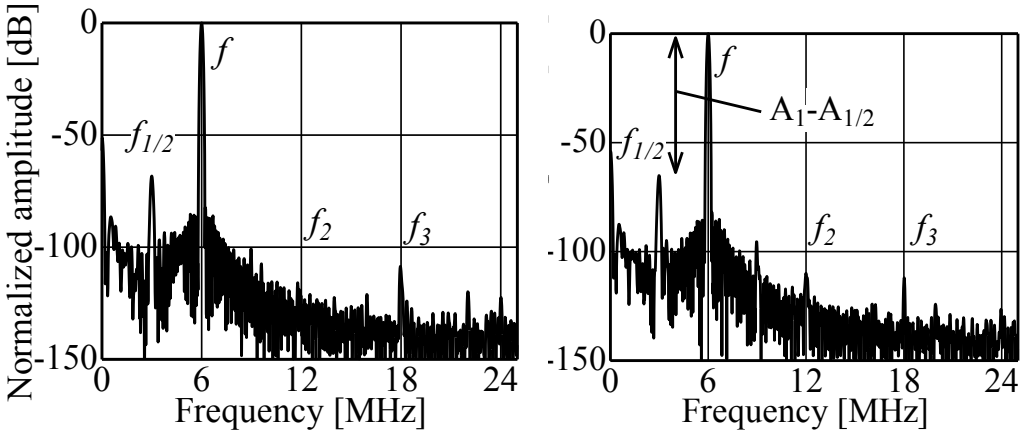

(c) 300V (d) 402V

Fig. 7. Input voltage versus relative subharmonic amplitude

for various contact pressures. (#1000 blocks with aluminum foil).

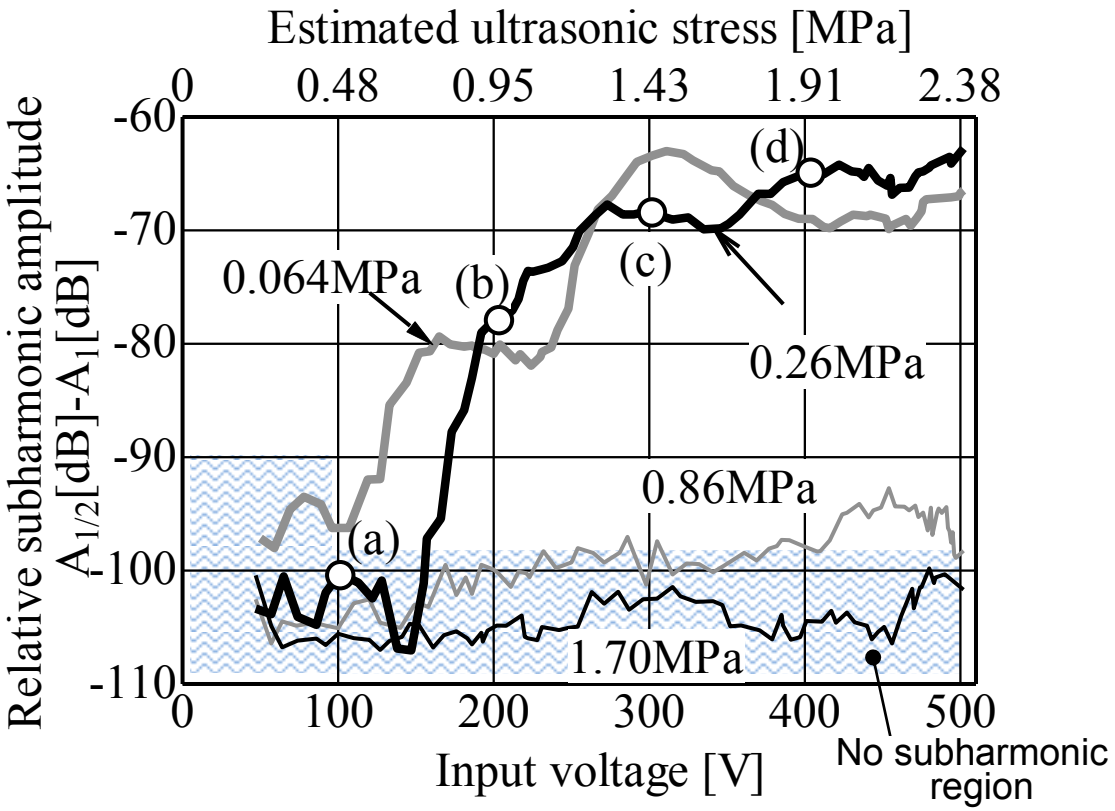

Fig. 8. Input voltage versus relative subharmonic amplitude for various surface roughnesses.（specimens with aluminum foil, contact pressure 0.064MPa）.

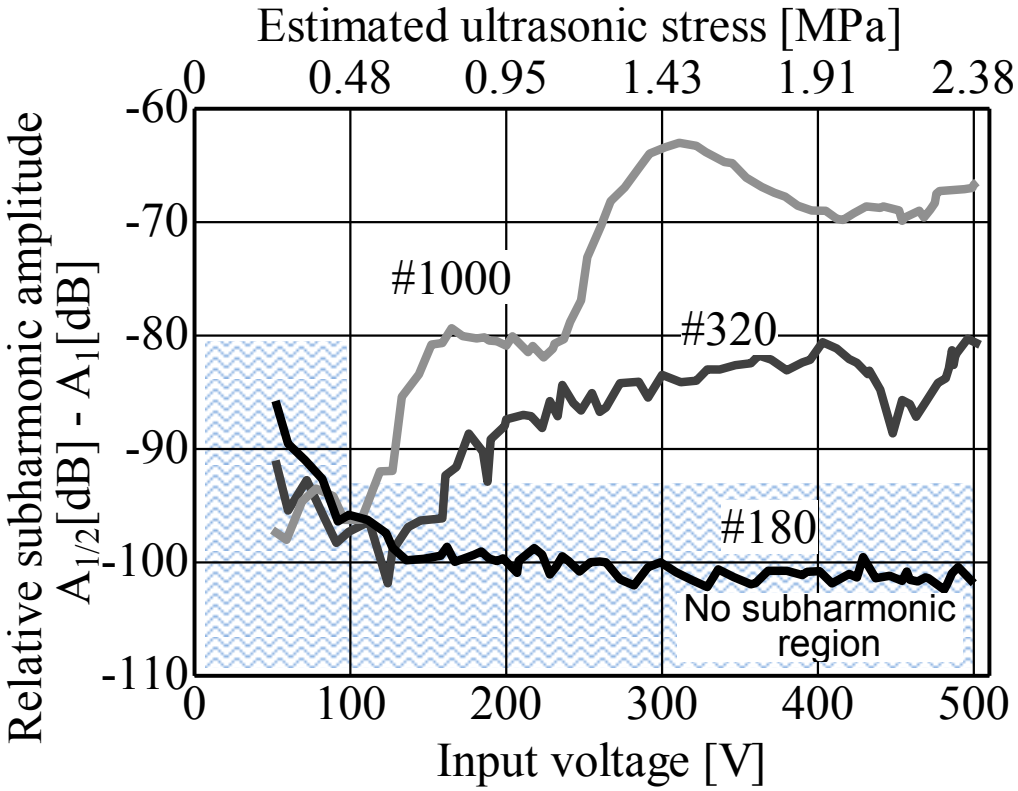

Fig. 9. Schematic figure of measurements of interface vibration.

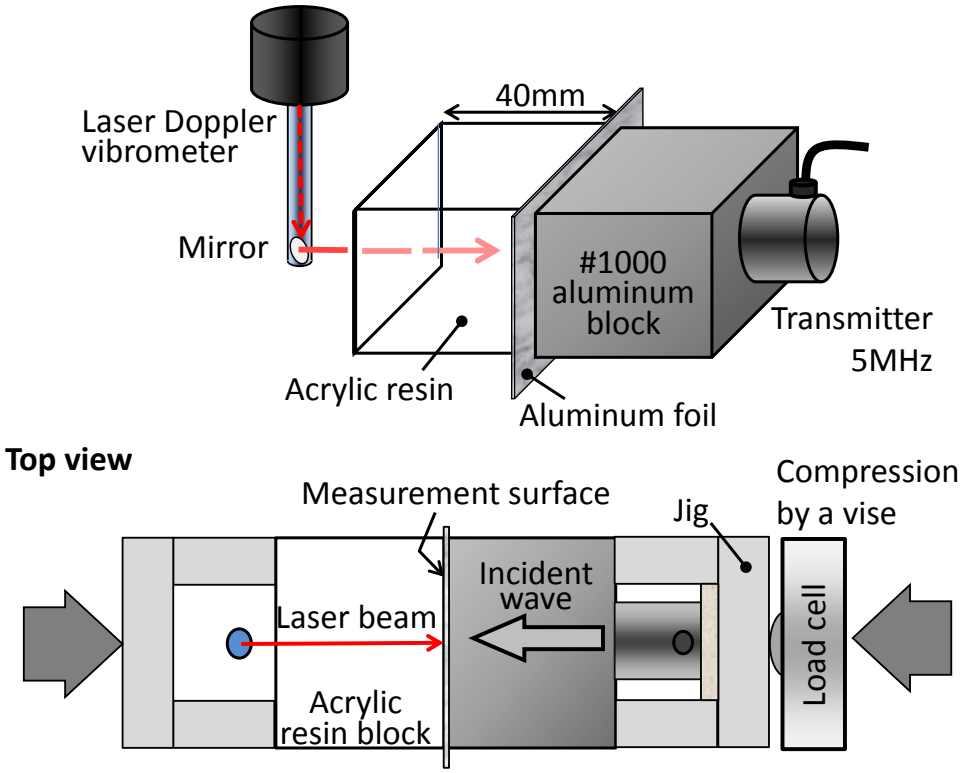

Fig. 10. Waveforms and amplitude spectra for various interface conditions.